Systems Analysis Modelling Simulation
Publication details, including instructions for authors and subscription information:
http://www.informaworld.com/smpp/title~content=t713649393

Discontinuous Fold Bifurcations

Remco I. Leine[a]; Dick H. van Campen[a]
[a] Department of Mechanical Engineering, Eindhoven University of Technology, Eindhoven, MB, The Netherlands

Online publication date: 29 October 2010

To cite this Article Leine, Remco I. and van Campen, Dick H.(2003) 'Discontinuous Fold Bifurcations', Systems Analysis Modelling Simulation, 43: 3, 321 — 332
To link to this Article: DOI: 10.1080/0232929031000119134
URL: http://dx.doi.org/10.1080/0232929031000119134

Systems Analysis Modelling Simulation
Vol. 43, No. 3, March 2003, pp. 321–332

Taylor & Francis
Taylor & Francis Group

DISCONTINUOUS FOLD BIFURCATIONS

REMCO I. LEINE* and DICK H. VAN CAMPEN

Department of Mechanical Engineering, Eindhoven University of Technology, P.O. Box 513, 5600 MB Eindhoven, The Netherlands

(Received 22 May 2000)

This article treats discontinuous fold bifurcations of periodic solutions of discontinuous system. It is shown how jumps in the fundamental solution matrix lead to jumps of the Floquet multipliers of periodic solutions. A Floquet multiplier of a discontinuous system can jump through the unit circle causing a discontinuous bifurcation. Numerical examples are treated which show discontinuous fold bifurcations. The discontinuous fold bifurcation can connect stable branches to branches with infinitely unstable solutions.

Keywords: Discontinuous; Bifurcation; Stick–slip; Dry friction

1. INTRODUCTION

The objective of this article is to explain how discontinuous fold bifurcations arise in systems with a discontinuous vector field.

During the last two decades many textbooks about bifurcation theory for smooth systems appeared and bifurcations of smooth vector fields are well understood [6,7,10,18,21]. However, little is known about bifurcations of discontinuous vector fields. Discontinuous dynamical systems arise due to physical discontinuities such as dry friction, impact and backlash in mechanical systems or diode elements in electrical circuits. Many papers deal with discontinuous systems [5,8,9,19,20,22–24]. Published bifurcation diagrams constructed from data obtained by brute force techniques only show stable branches of periodic solutions, whereas those made by path-following techniques do show bifurcations to unstable branches but the bifurcations behave smoothly and are not discontinuous.

Andronov *et al*. [2] treat periodic solutions of discontinuous systems. They revealed many aspects of discontinuous systems but did not treat discontinuous bifurcations with regard to Floquet theory.

The current article shows two examples of discontinuous fold bifurcations and explains how they come into being through Floquet theory. The first example is a trilinear spring system which shows a discontinuous fold bifurcation connecting a

*Corresponding author. E-mail: r.i.leine@tue.nl

ISSN 0232-9298 print: ISSN 1029-4902 online © 2003 Taylor & Francis Ltd
DOI: 10.1080/0232929031000119134

stable branch to an unstable branch. A stick–slip system is treated in the second example. The discontinuous fold bifurcation connects a stable branch to an infinitely unstable branch.

2. TRILINEAR SPRING SYSTEM

In this section we will treat a discontinuous fold bifurcation arising in a trilinear spring system (Fig. 1).

The forced oscillation of a damped mass on a spring with cubic term leads to the Duffing equation [6,7,16,17]. The Duffing equation is the classical example where the backbone curve of the harmonic peak is bended and two folds (also called turning point bifurcations) are born. In our example, we will consider a similar mass–spring–damper system, where the cubic spring is replaced by a trilinear spring. Additionally, trilinear damping is added to the model. The trilinear damping will turn out to be essential for the existence of a *discontinuous* fold bifurcation.

The model is very similar to the model of Natsiavas [14,15], but the transitions from contact with the support to no contact are different from Natsiavas. The model of Natsiavas switches as the position of the mass passes the contact distance (in both transition directions). In our model, contact is made when the position of the mass passes the contact distance, and contact is lost when the contact force becomes zero.

We consider the system depicted in Fig. 1. The model has two supports on equal contact distances x_c. The supports are first-order systems which relax to their original state if there is no contact with the mass. If we assume that the relaxation time of the supports is much smaller than the time interval between two impacts, we can neglect the free motion of the supports. It is thus assumed that the supports are at rest at the moment of impact. This is not an essential assumption but simplifies our treatment

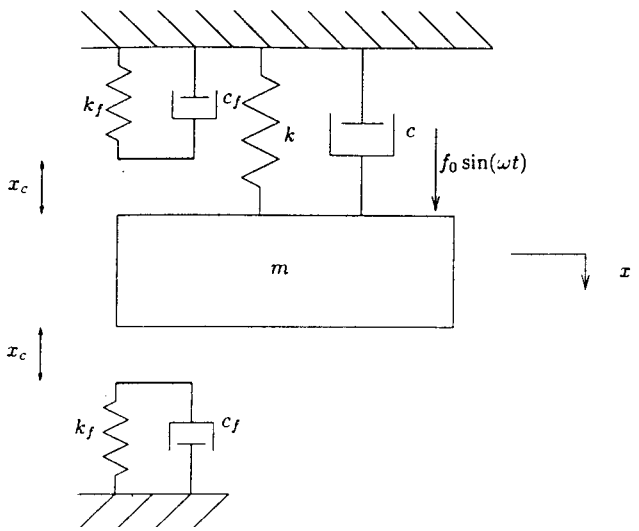

FIGURE 1 Trilinear system.

as the system reduces to a second-order equation. The second-order differential equation of this system is

$$m\ddot{x} + C(\dot{x}) + K(x) = f_0 \sin(\omega t), \tag{1}$$

where

$$K(x) = \begin{cases} kx & [x, \dot{x}]^T \in V_- \\ kx + k_f(x - x_c) & [x, \dot{x}]^T \in V_{+1} \\ kx + k_f(x + x_c) & [x, \dot{x}]^T \in V_{+2} \end{cases} \tag{2}$$

is the trilinear restoring force and

$$C(\dot{x}) = \begin{cases} c\dot{x} & [x, \dot{x}]^T \in V_- \\ (c + c_f)\dot{x} & [x, \dot{x}]^T \in V_{+1} \cup V_{+2} \end{cases} \tag{3}$$

is the trilinear damping force. The state space is divided into three subspaces V_-, V_{+1} and V_{+2} (Fig. 2).

If the mass is in contact with the lower support, then the state is in space V_{+1}

$$V_{+1} = \{[x, \dot{x}]^T \in \mathbb{R}^2 | x > x_c, k_f(x - x_c) + c_f\dot{x} \geq 0\},$$

whereas if the mass is in contact with the upper support, then the state is in space V_{+2}

$$V_{+2} = \{[x, \dot{x}]^T \in \mathbb{R}^2 | x < -x_c, k_f(x + x_c) + c_f\dot{x} \leq 0\}.$$

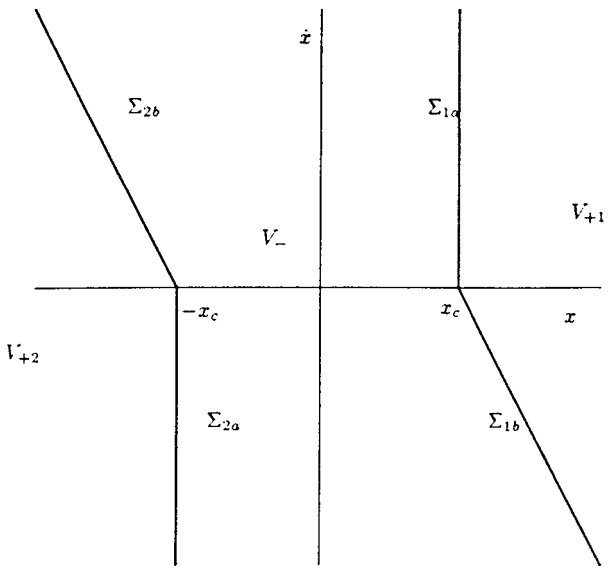

FIGURE 2 Subspaces of the trilinear system.

If the mass is not in contact with one of the supports, then the state is in space V_- defined by

$$V_- = \{[x, \dot{x}]^T \in \mathbb{R}^2 | x \notin (V_{+1} \cup V_{+2})\}.$$

The hyperplane Σ_1 between V_- and V_{+1} consists of two parts Σ_{1a} and Σ_{1b}. The part Σ_{1n} is defined by the indicator equation

$$h_{1a} = x - x_c = 0, \tag{4}$$

which defines the transition from V_- to V_{+1} because contact is made when x becomes larger than x_c. The part Σ_{1a} is defined by the indicator equation

$$h_{1b} = k_f(x - x_c) + c_f\dot{x} = 0, \tag{5}$$

which defines the transition from V_{+1} back to V_- as contact is lost when the support-force becomes zero (the support can only push, not pull on the mass). Similarly, the hyperplane Σ_2 between V_- and V_{+2} consists of two parts Σ_{2a} and Σ_{2b} defined by the indicator equations

$$h_{2a} = x + x_c = 0, \tag{6}$$

$$h_{2b} = k_f(x + x_c) + c_f\dot{x} = 0. \tag{7}$$

Discontinuous systems exhibit discontinuities (or 'saltations'/'jumps') in the time evolution of the fundamental solution matrix.

The jumps occur when the solution crosses a hyperplane of discontinuity and can be described by a saltation matrix $\underline{S}$

$$\underline{\Phi}(t_{p+}, t_0) = \underline{S}\,\underline{\Phi}(t_{p-}, t_0), \tag{8}$$

where $\underline{\Phi}(t_{p-}, t_0)$ is the fundamental solution matrix before the jump and $\underline{\Phi}(t_{p+}, t_0)$ after the jump which occurs at $t = t_p$. The saltation matrix $\underline{S}$ can be expressed as

$$\underline{S} = \underline{I} + \frac{\left(\underset{\sim}{f}_{p+} - \underset{\sim}{f}_{p-}\right)^{n\,t}}{\underset{\sim}{n}^T \underset{\sim}{f}_{p-} + (\partial h/\partial t)(t_p, \underset{\sim}{x}(t_p))}, \tag{9}$$

where $\underset{\sim}{n}$ is the normal to the hyperplane

$$\underset{\sim}{n} = \underset{\sim}{n}(t, \underset{\sim}{x}) = \mathrm{grad}(h(t, \underset{\sim}{x}(t)). \tag{10}$$

The construction of saltation matrices is due to Aizerman and Gantmakher [1] and treated in [3,12,13]. The saltation matrices for each hyperplane are

$$\underline{S}_{1a} = \begin{bmatrix} 1 & 0 \\ -\frac{c_f}{m} & 1 \end{bmatrix}, \tag{11}$$

$$\underline{S}_{1b} = \underline{I}, \tag{12}$$

$$S_{2a} = \begin{bmatrix} 1 & 0 \\ -\frac{c_f}{m} & 1 \end{bmatrix}, \tag{13}$$

$$\underline{S}_{2b} = \underline{I}. \tag{14}$$

The hyperplanes Σ_1 and Σ_2 are non-smooth. The saltation matrices are not each others inverse, $\underline{S}_{1a} \neq \underline{S}_{1b}^{-1}$ and $\underline{S}_{2a} \neq \underline{S}_{2b}^{-1}$. This will turn out to be essential for the existence of a discontinuous bifurcation. Note that the saltation matrices are independent of the stiffness k and reduce to the identity matrix if $c_f = 0$.

The response diagram of the trilinear system is shown in Fig. 3 for varying forcing frequencies with the amplitude A of x on the vertical axis. Stable branches are indicated by solid lines and unstable branches by dashed–dotted lines. The parameter values are given in Appendix A.

There is no contact with the support for amplitudes smaller than x_c and the response curve is just the linear harmonic peak. For amplitudes above x_c there will be contact with the support which will cause a hardening behaviour of the response curve. The backbone curve of the peak bends to the right like the Duffing system with a hardening spring. The amplitude becomes equal to x_c twice at $\omega = \omega_A$ and $\omega = \omega_B$, on both sides of the peak, and corners of the response curve can be seen at these points. The orbit touches the corners of Σ_1 and Σ_2 for $A = x_c$.

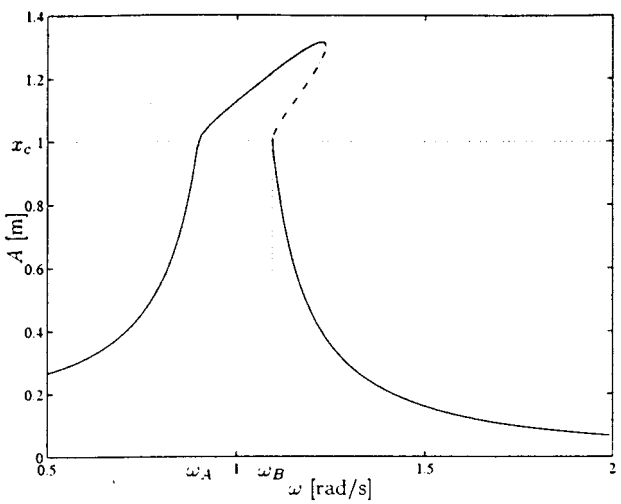

FIGURE 3 Response diagram of trilinear spring system.

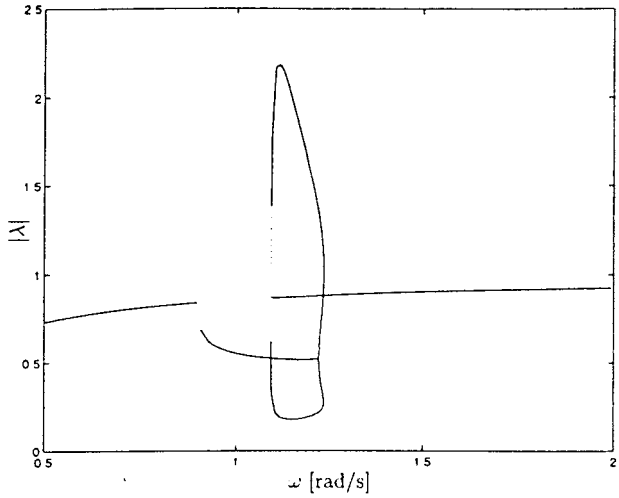

FIGURE 4 Floquet multipliers.

The magnitude of the Floquet multipliers is shown in Fig. 4. The two Floquet multipliers are complex conjugate (with the same magnitude) for $A < x_c$. The orbit touches the two hyperplanes at $A < x_c$ and the fundamental solution matrix will jump as follows from the saltation matrices. The eigenvalues of the fundamental solution matrix, which are known as the Floquet multipliers, will therefore jump (indicated by dotted lines in Fig. 4). The Floquet multipliers are not singular valued at the bifurcation point (as is the case for smooth systems) but are set-valued.

The pair of Floquet multipliers jumps at ω_A but does not jump through the unit circle. The set-valued Floquet multiplier remains within the unit circle. The stable branch thus remains stable. However, at $\omega = \omega_B$ the complex pair jumps to two distinct real multipliers, one with a magnitude bigger than one. A Floquet multiplier thus jumped through the unit circle. This set-valued Floquet multiplier passed the unit circle through $+1$ causing a *discontinuous fold bifurcation*.

Damping of the support is essential for the existence of this discontinuous fold bifurcation. For $c_f = 0$, all saltation matrices would be equal to the identity matrix and the corner between Σ_{1a} and Σ_{1b} would disappear (and also between Σ_{2a} and Σ_{2b}); thus no discontinuous bifurcation could take place and the fold bifurcation would be smooth. The model of Natsiavas [14,15] did not contain a *discontinuous* fold bifurcation because the transitions were modelled such that $\underline{S}_{1a} = \underline{S}_{1b}^{-1}$ and $\underline{S}_{2a} = \underline{S}_{2b}^{-1}$. The saltation matrices will cancel each other out if they are each other inverse. A corner of hyperplanes with saltation matrices which are not each others inverse is therefore essential (but not sufficient) for the existence of a discontinuous bifurcation.

3. STICK–SLIP SYSTEM

In the preceding subsection we studied a discontinuous fold bifurcation, where a Floquet multiplier jumped over the unit circle to a finite value. In this subsection we will study a discontinuous fold bifurcation where the Floquet multiplier jumps to infinity. This results in an infinitely unstable periodic solution.

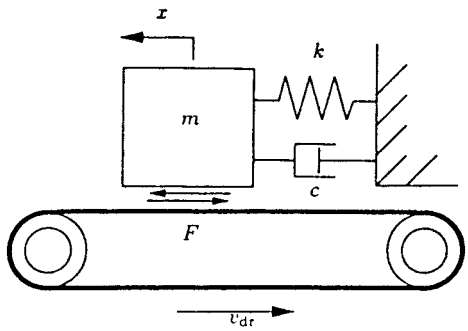

FIGURE 5 1-DOF model with dry friction.

We consider the block-on-belt model depicted in Fig. 5 with the parameter values given in Appendix B. The state equation of this autonomous system reads

$$\dot{\underset{\sim}{x}} = \underset{\sim}{f}(\underset{\sim}{x}) = \begin{bmatrix} \dot{x} \\ -\frac{k}{m}x - \frac{c}{m}\dot{x} + \frac{F}{m} \end{bmatrix}, \tag{15}$$

where $\underset{\sim}{x} = [x \quad \dot{x}]^T$ and the friction force F is given by

$$F(v_{\text{rel}}, x) = \begin{cases} -F_{\text{slip}} \operatorname{sgn} v_{\text{rel}}, & v_{\text{rel}} \neq 0 \quad \text{slip} \\ \min(|kx + c\dot{x}|, F_{\text{stick}}) \operatorname{sgn} kx. & v_{\text{rel}} = 0 \quad \text{stick} \end{cases} \tag{16}$$

The maximum static friction force is denoted by F_{stick} and $v_{\text{rel}} = \dot{x} - v_{\text{dr}}$ is the relative velocity. The constitutive relation for F is known as the *signum model with static friction point*.

This model permits analytical solutions for $c = 0$ due to its simplicity but it is not directly applicable in numerical analysis. The relative velocity will most likely not be exactly zero in digital computation. Instead, an adjoint *switch model* [11] will be studied which is discontinuous but yields a set of ordinary (and non-stiff !) differential equations. The state equation for the switch model reads

$$\dot{\underset{\sim}{x}} = \begin{cases} \begin{bmatrix} \dot{x} \\ -\frac{k}{m}x - \frac{c}{m}\dot{x} - \frac{F_{\text{slip}}}{m} \operatorname{sgn} v_{rel} \end{bmatrix} & |v_{\text{rel}}| > \eta \text{ or } |kx + c\dot{x}| > F_{\text{stick}} \\ \begin{bmatrix} v_{\text{dr}} \\ -v_{\text{rel}}\sqrt{\frac{k}{m}} \end{bmatrix} & |v_{\text{rel}}| < \eta \text{ and } |kx + c\dot{x}| < F_{\text{stick}} \end{cases} \tag{17}$$

A region of near-zero velocity is defined as $|v_{\text{rel}}| < \eta$ where $\eta \ll v_{\text{dr}}$. Thus, the space R^2 is divided in three subspaces V, W and D as indicated in Fig. 6. The boundaries between the subspaces are denoted by bold lines. The small parameter η is enlarged to make D visible.

The equilibrium solution of system 15 is given by

$$\underset{\sim}{x}\, eq = \begin{bmatrix} \frac{F_{\text{slip}}}{k} \\ 0 \end{bmatrix} \tag{18}$$

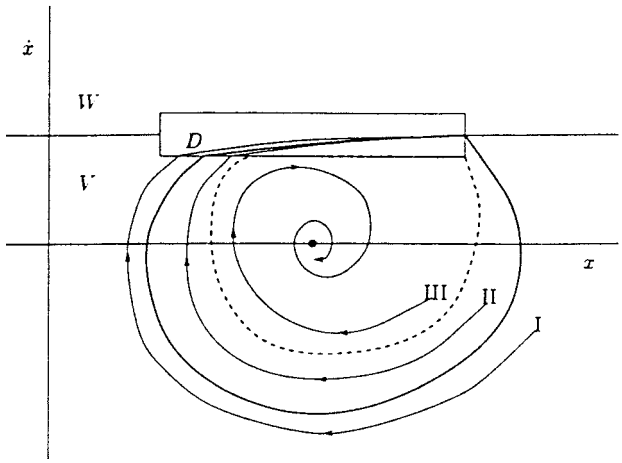

FIGURE 6 Phase plane.

and is stable for positive damping ($c > 0$).

The model also exhibits stable periodic stick–slip oscillations. The saltation matrix $\underline{S}_\alpha$ for the transition from slip to stick is given by [12]

$$\underline{S}_\alpha = \begin{bmatrix} 1 & 0 \\ 0 & 0 \end{bmatrix}, \tag{19}$$

which is singular. The fundamental solution matrix will thus also be singular as the stable periodic oscillation passes the stick state. The saltation matrix $\underline{S}_3$ for the transition from stick to slip is given by

$$\underline{S}_3 = \begin{bmatrix} 1 & 0 \\ -\frac{\Delta F}{m v_{\mathrm{dr}}} & 1 \end{bmatrix}, \tag{20}$$

with $\Delta F = F_{\mathrm{stick}} - F_{\mathrm{slip}}$.

The periodic solution has two Floquet multipliers, of which one is always equal to unity as the system is autonomous. The singularity of the fundamental solution matrix implies that the remaining Floquet multiplier has to be equal to zero, independent of any system parameter. The Floquet multipliers of the stable periodic solution of this system are thus $\lambda_{\mathrm{stable}} = (1,0)$.

The stable limit cycle is sketched in the phase plane in Fig. 6 (bold line). The equilibrium position is also stable and indicated by a dot. The space D is enlarged in Fig. 6 to make it visible but is infinitely small in theory and is taken very small in numerical calculations [11,12].

A trajectory outside the stable limit cycle, like trajectory I in Fig. 6, will spiral inwards to the stable limit cycle and reach the stick–phase D. The stick–phase will bring the trajectory exactly on the stable limit cycle as it is infinitely small. Every point in D is thus part of the basin of attraction of the stable limit cycle.

Trajectory II starts inside the stable limit cycle and spirals around the equilibrium position and hits D where-after it is on the stable limit cycle. But a trajectory inside

the stable limit cycle might also spiral around the equilibrium position and not reach the stick-phase D (trajectory III). It will then be attracted to the equilibrium position.

A trajectory inside the stable limit cycle can thus spiral outwards to the stable limit cycle, like trajectory II, or inwards to the equilibrium position (trajectory III). Consequently, there must exist a boundary of attraction between the two attracting limit sets. This boundary is the unstable limit cycle sketched by a dashed line in Fig. 6. Whether a flow is attracted to the stable limit cycle or to the equilibrium point depends on the attainment of the trajectory to D. The unstable limit cycle is thus defined by the trajectory in V which hits the border of D tangentially. Another part of the unstable limit cycle is along the border of D as trajectories in D will attract ot the stable limit cycle and just outside D to the equilibrium poition. This part of the unstable limit cycle along the border of D is has a vector field which is repulsing on both sides of the border. The theory of Filippov gives a generalized solution of systems with a discontinuous right-hand side [4,12]. If the vector field on one side of a hyperplane of discontinuity is pushing to the hyperplane and on the other side from the hyperplane, then every trajectory will intersect the hyperplane transversally. If the vector field is pushing to the hyperplane on both sides then there exists a unique solution along the hyperplane. This is called an *attraction sliding mode*. If the vector field is repulsing from both sides of the hyperplane then there exists a solution along the hyperplane which is not unique. This is called a *repulsion sliding mode*.

The vector field solution on either side of the border of D is repulsing from it. It is thus a repulsion sliding mode. The solution starting from a point on a repulsion sliding mode is not unique as follows from the theory of Filippov. This causes the unstable solution to be infinitely unstable. As the solution is infinitely unstable, it is not possible to calculate it in forward time. However, calculation of the solution in backward time is possible. The vector field in backward time is identical to forward time but opposite in direction. The repulsion sliding mode in forward time will turn into an attraction sliding mode in backward time. The solution starting from a point on the unstable limit cycle will move counter-clockwise in the phase-plane in backward time and hit the border of D. It will slide along the border of D until the vector field in V becomes parallel to D, and will then bend off in V. Any solution starting from a point close to that starting point will hit D and leave D at exactly the same point. Information about where the solution came from is thus lost through the attraction sliding mode. In other words: the saltation matrix of the transition from V to D during backward time is singular. The fundamental solution matrix will thus be singular in backward time because it contains an attraction sliding mode. The Floquet multipliers of the unstable limit cycle in backward time are therefore 1 and 0. The Floquet multipliers in forward time must be their reciprocal values. The second Floquet multiplier is thus infinity, $\lambda_{\text{unstable}} = (1, \infty)$, which of course must hold for an infinitely unstable periodic solution.

The bifurcation diagram of the system is shown in Fig. 7 with the velocity of the belt v_{dr} as control parameter and the amplitude A on the vertical axis. The equilibrium branch and the stable and unstable periodic branches are depicted. The unstable branch is of course located between the stable periodic branch and the equilibrium branch as can be inferred from Fig. 6. The stable and unstable periodic branches are connected through a fold bifurcation point. The second Floquet multiplier jumps from $\lambda = 0$ to $\lambda = \infty$ at the bifurcation point. This set-valued Floquet multiplier thus passes the unit circle at $+1$. The fold bifurcation is therefore a discontinuous fold bifurcation. The fold bifurcation occurs when v_{dr} is such that a flow which leaves the stick-phase

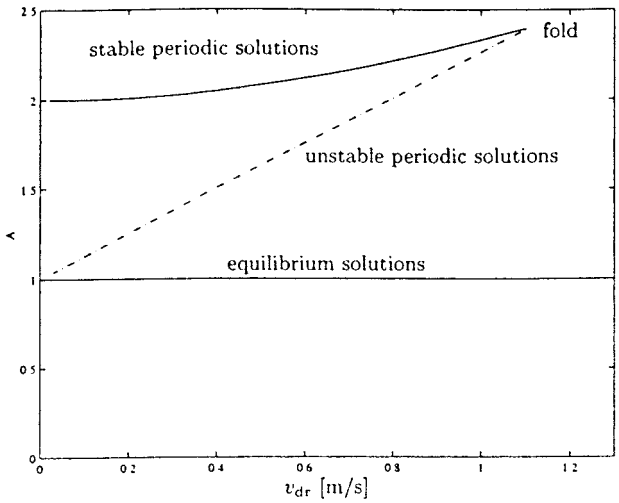

FIGURE 7 Bifurcation diagram of the block-on-belt model.

D, transverses V, and hits D tangentially (like the unstable periodic solution). The stable and unstable periodic solutions coincide at this point. Note that there exists again a corner of hyperplanes at this point as was the case in the previous section. The saltation matrices are not each others inverse, $\underline{S}_\alpha \underline{S}_\beta \neq \underline{I}$, which is essential for the existence of a discontinuous bifurcation.

A similar model was studied by Van de Vrande *et al.* [24] with a very accurately smoothed friction curve. The stable branch was followed for increasing v_{dr} but the fold bifurcation could not be rounded to proceed on the unstable branch. As the unstable branch is infinitely unstable in theory, it is extremely unstable for the smoothed system. The branch can thus not be followed in forward time if the friction model is approximated accurately.

The stable branch in Fig. 7 was followed in forward time up to the bifurcation point. The path-following algorithm was halted and restarted in backward time to follow the unstable branch.

This section showed that infinitely unstable periodic solutions come into being through repulsion sliding modes. Filippov theory turns out to be essential for the understanding of infinitely unstable periodic solutions. Infinitely unstable periodic solutions and their branches can be found through backward integration. Smoothing of a discontinuous model is not sufficient to obtain a complete bifurcation diagram of a discontinuous system as infinitely unstable branches cannot be found.

CONCLUSIONS

It was shown in this article that discontinuous vector fields lead to jumps in the fundamental solution matrix if a control parameter is varied. It turned out that a double intersection of a non-smooth hyperplane is necessary to cause a jump of the fundamental solution matrix. These jumps may lead to set-valued Floquet multipliers. A discontinuous bifurcation is encountered if a set-valued Floquet multiplier crosses the unit circle.

An example with a trilinear spring demonstrated two jumps of the Floquet multipliers, one causing a discontinuous fold bifurcation.

An example of a stick–slip system showed that the Floquet multiplier can also jump to infinity. The discontinuous fold bifurcation connects a stable branch to an infinitely unstable branch. The unstable limit cycle can be understood by Filippov's theory. Infinitely unstable periodic solutions come into being through repulsion sliding modes and can be found through backward integration. Branches of infinitely unstable periodic solutions can be continued with pseudo-arclength continuation based on shooting with backward integration. Bifurcation to infinitely unstable periodic solutions lead to complete failure of the classical smoothing method to investigate discontinuous systems.

The theory of bifurcations of periodic solutions has been extended in the paper to discontinuous bifurcation. Only fold bifurcations were discussed. A more complete theory of the bifurcation in discontinuous systems is presented in [12].

References

[1] M.A. Aizerman and F.R. Gantmakher (1958). On the stability of periodic motions. *Journal of Applied Mathematics and Mechanics* (translated from Russian), pp. 1065–1078.

[2] A.A. Andronov, A.A. Vitt and S.E. Khaikin (1987). *Theory of Oscillators*, Dover Publications, New York.

[3] S.F. Bockman (1991). Lyapunov exponents for systems described by differential equations with discontinuous right-hand sides. In: *Proceedings of the American Control Conference*, pp. 1673–1678.

[4] A.F. Filippov (1964). Differential equations with discontinuous right-hand side. *American Mathematical Society Translations*, Series 2, **42**, 199–231.

[5] U. Galvanetto, S.R. Bishop and L. Briseghella (1995). Mechanical stick-slip vibrations. *International Journal of Bifurcation and Chaos*, **5**(3), 637–651.

[6] J. Guckenheimer and P. Holmes (1983). Nonlinear oscillations, dynamical systems, and bifurcations of vector fields. *Applied Mathematical Sciences*, Vol. 42, Springer-Verlag, New York.

[7] P. Hagedorn, (1988). *Non-Linear Oscillations*, Oxford Engineering Science Series 10, Oxford.

[8] R.A. Ibrahim (1994a). Friction-induced vibration, chatter, squeal and, chaos; part I: mechanics of contact and friction. *ASME Applied Mechanics Reviews*, **47**(7), 209–226.

[9] R.A. Ibrahim (1994). Friction-induced vibration, chatter, squeal and, chaos; Part II: Dynamics and modeling. *ASME Applied Mechanics Review*, **47**(7), 227–253.

[10] Y.A. Kuznetsov (1995). Elements of Applied Bifurcation Theory, *Applied Mathematical Sciences*, Vol. 112, Springer-Verlag, New York.

[11] R.I. Leine, D.H. Van Campen, A. De Kraker and L. Van den Steen (1998). Stick-slip vibrations induced by alternate friction models. *Nonlinear Dynamics*, **16**(1), 41–54.

[12] R.I. Leine, D.H. Van Campen and B.L. Van de Vrande (2000). Bifurcation in nonlinear discontinuous systems. *Nonlinear Dynamics*, **23**(2), 105–164.

[13] P.C. Müller (1995). Calculation of Lyapunov exponents for dynamic systems with discontinuities. *Chaos, Solitons and Fractals*, **5**(9), 1671–1681.

[14] S. Natsiavas (1989). Periodic response and stability of oscillators with symmetric trilinear restoring force. *Journal of Sound and Vibration*, **134**(2), 315–331.

[15] S. Natsiavas and H. Gonzalez (1992). Vibration of harmonically excited oscillators with asymmetric constraints. *ASME Journal of Applied Mechanics*, **59**, 284–290.

[16] A.H. Nayfeh and B. Balachandran (1995). Analytical, Computational, and Experimental Methods. *Applied Nonlinear Dynamics*, Wiley, New York.

[17] A.H. Nayfeh and D.T. Mook (1979). *Nonlinear Oscillations*, Wiley, New York.

[18] T.S. Parker and L.O. Chua (1989). *Practical Numerical Algorithms for Chaotic Systems*. Springer-Verlag, New York.

[19] K. Popp (19992). Some model problems showing stick-slip motion and chaos, In: R.A. Ibrahim and A. Soom (Eds.), *ASME WAM*, *Proc. Symp. on Friction Induced Vibration*, *Chatter*, *Squeal*, *and Chaos*, Vol. **49**, pp. 1–12, ASME New York.

[20] K. Popp, N. Hinrichs and M. Oestreich (1995). Dynamical behaviour of a friction oscillator with simultaneous self and external excitation, In: *Sādhāna: Academy Proceedings in Engineering Sciences*, Vol. 20, Part 2–4, pp. 627–654, Indian Academy of Sciences, Bangalore, India.

[21] R. Seydel (1994). Practical bifurcation and stability analysis; from equilibrium to chaos. *Interdisciplinary Applied Mathematics*, Springer-Verlag, New York.
[22] P. Stelter (1992). Nonlinear vibrations of structures induced by dry friction. *Nonlinear Dynamics*, **3**, 329–345.
[23] P. Stelter and W. Sextro (1991). Bifurcations in dynamical systems with dry friction. *International Series of Numerical Mathematics*, **97**, 343–347.
[24] B.L. Van de Vrande, D.H. Van Campen and A. De Kraker (1997). Some aspects of the analysis of stick-slip vibrations with an application to drillstrings. In: *Proceedings of ASME Design Engineering Technical Conference*, 16th Biennial Conference on Mechanical Vibration and Noise, DETC/VIB-4109, published on CD-ROM, September 14–17, 8pp., Sacramento.

APPENDIX A: TRILINEAR SPRING SYSTEM

$$\begin{aligned} m &= 1\,\mathrm{kg} \\ k &= 1\,\mathrm{N/m} \\ k_f &= 4\,\mathrm{N/m} \\ f_0 &= 0.2\,\mathrm{N} \\ c &= 0.5\,\mathrm{N/ms} \\ x_c &= 1\,\mathrm{m} \\ c_f &= 0.5\,\mathrm{N/ms} \end{aligned}$$

APPENDIX B: STICK–SLIP SYSTEM

$$\begin{aligned} k &= 1\,\mathrm{N/m} \\ m &= 1\,\mathrm{kg} \\ F_{\mathrm{slip}} &= 1\,\mathrm{N} \\ \eta &= 10^{-4}\mathrm{m/s} \\ c &= 0.1\,\mathrm{N\,s/m} \\ v_{dr} &= 1\,\mathrm{m/s} \\ F_{\mathrm{slip}} &= 2\,\mathrm{N} \end{aligned}$$